

Adsorption and Self-Assembly of Corrosion Inhibitors on Metallic Surfaces Studied Using Molecular Simulations

Xueying Ko, Sumit Sharma
Department of Chemical and Biomolecular Engineering
Ohio University
Athens, OH, 45701
USA

ABSTRACT

Organic corrosion inhibitors are widely used in oil and gas industry to mitigate the internal corrosion of oil and gas pipelines. These inhibitor molecules are known to self-assemble and form a protective layer at the metal-water interfaces. In this work, we have studied adsorption and self-assembly of inhibitor molecules of different chemistries and geometry on polar surfaces using classical molecular dynamics simulations by employing a coarse-grained model. We show that (a) hydrophobic interactions between inhibitor tails play an important role in their adsorption and self-assembly on surfaces, (b) the morphology of the adsorbed film is dictated by the molecular geometry of inhibitors, and (c) metal-polar head group interactions change the nature of adsorbed corrosion inhibitor films. We also show that in an oil saturated aqueous phase, inhibitor molecules have a tendency to entrain oil molecules into the adsorbed films and this process dramatically changes their adsorbed morphology.

Key words: corrosion inhibitors, adsorption, molecular simulation

INTRODUCTION

Oil and gas pipelines are prone to internal corrosion.¹ To mitigate internal corrosion, a popular approach is to use corrosion inhibitors. Corrosion inhibitors are injected into the oil flow stream at concentration levels of parts-per-million. Corrosion inhibitor formulations comprise of a mixture of surfactants.^{2, 3} Surfactant molecules are amphiphilic in nature, consisting of a hydrophilic head (polar) group and a hydrophobic (nonpolar) tail. The hydrophilic heads are either non-ionic or ionic functional groups, while the hydrophobic tails are hydrocarbon chains comprising of usually 6 to 22 carbon atoms. The corrosion inhibition properties of these molecules are closely linked to their tendency to adsorb at the metal-water interface.⁴ Some examples of the widely used inhibitor molecules in oil and gas industry are imidazole, quaternary ammonium, amide and amidoamine based surfactants because of their low toxicity, low cost, are high efficacy.⁵⁻⁷

Numerous experimental studies using saturation adsorption data,² Electrochemical Impedance Spectroscopy (EIS),^{8,9} Second Harmonic Generation Laser Scattering,¹⁰ and Atomic Force

Microscopy(AFM) ¹¹ indicate that these corrosion inhibitor molecules mitigate corrosion by their self-assembly into monolayers or micelles onto metal surfaces upon adsorption. While experimental observations do suggest that corrosion inhibition is correlated to surface coverage of inhibitor molecules, the mechanism by which adsorbed inhibitor molecules mitigate corrosion is poorly understood. We need to understand how factors, such as molecular structure of inhibitor molecules, geometries of inhibitor molecules and the metal-inhibitor interaction changes the stability and the mechanism of self-assembled monolayer (SAM) formation. Also, previous studies have focused on evaluating corrosion inhibition efficiency in the aqueous phase devoid of oil molecules. The role of oil, if any, on the inhibition efficiency of these molecules has not been explored.

In this study, we have performed molecular simulations of corrosion inhibitor molecules modeled using a coarse-grained model to understand how different molecular structures, metal-inhibitor interactions and presence of oil molecules affects the adsorption behavior of corrosion inhibitors.

EXPERIMENTAL PROCEDURE

Coarse-grained Modeling and Simulation System Setup: Adsorption and self-assembly are collective phenomena wherein interactions between a large number of molecules dictate the overall process. In general, collective behavior of molecules involves long length- and timescales. Thus, these phenomena are studied using coarse-grained modeling techniques. In coarse-grained models, chemical identities of individual atoms are ignored, and instead, groups of atoms are represented by "coarse-grained beads", and different potential functions were employed to represent the interactions between the beads of the molecules.

In our system, corrosion inhibitor molecules are represented by a coarse-grained (CG) bead-spring model described in detail in a previous work.¹² Briefly, one terminal bead represents the polar head group and a linear chain of beads represents the alkyl tail of the molecules. The polar head beads are strongly attracted to the metal surface, and the hydrocarbon tail beads have hydrophobic interactions between themselves. Oil molecules in our system are represented by hydrophobic beads in a linear chain. Bonded interactions between the connected beads within a molecule and the angular potentials between adjacent bonds in a molecule are modeled as harmonic potentials. The equilibrium angle of the angular potential is 180°. Water molecules are not explicitly included in the system. The effect of water molecules is implicitly included by performing Langevin dynamics simulation. In Langevin dynamics, all beads in the system experience a Gaussian random force as well as a drag force proportional to their velocity but in the direction opposite of the velocity. These two forces effectively mimic presence of solvent molecules. Interactions between the tail beads of inhibitor molecules, between the inhibitor tail beads and the oil beads and between the oil beads are hydrophobic interactions, and are modeled via Lennard-Jones (LJ) potential with the length parameter σ and the potential well-depth of ϵ . The parameter ϵ determines the strength of attractive interaction and the parameter σ is a measure of effective diameter of the bead. Interactions between the polar beads and the hydrophobic beads are modeled by purely repulsive Weeks-Chandler-Anderson (WCA) potential.¹³ WCA potential is a truncated and shifted LJ potential that includes only the repulsive part of LJ potential, with the LJ length parameter σ_p determines the effective diameter of the polar bead. The rationale of using this repulsive WCA potential for polar beads is that the polar groups in an aqueous environment have similar interactions with water molecules and other polar and hydrophobic groups. As a result, there is no net attraction between different polar groups or between polar and hydrophobic groups. The metal surface is represented by a smooth, two-dimensional surface covering the bottom face of the simulation box at $Z=0$. The strong attractive interactions between polar head beads and the surface are modeled via a 9-3 potential with the well-depth of ϵ_s . A 9-3 potential is obtained by integrating LJ potential over a semi-infinite slab. The hydrophobic beads have only repulsive, hard sphere interactions with the surface. The simulation box is periodic in the X and Y dimensions. To keep a constant simulation volume, reflective boundary conditions are applied to all beads at the side opposite of the $Z = 0$ surface of the simulation box.

All quantities are defined using reduced units in this study. In reduced units, the units of energy, mass, length are defined in such a way so as to save computational costs and can easily be converted to real units. In this system, the unit of energy is taken as thermal energy, $K_B T$ (K_B is Boltzmann constant and T is the temperature), which is set to 1. The potential well-depth, ϵ has units of energy, and therefore is specified with respect to $K_B T$. For instance, an $\epsilon=0.5$ implies that the potential well-depth is half of the thermal energy. The mass of each bead is set to 1, and the size of each hydrophobic bead, σ , is set to 1 in reduced units. More details on reduced units can be found in our previous publication.¹⁴

Simulation Details: Langevin dynamics simulations are performed to study the adsorption behavior of corrosion inhibitor and oil molecules on the surface. In Langevin dynamics, the motion of molecules is modeled to mimic their interactions with solvent molecules. The LJ well-depth parameter for the overall interaction between hydrophobic beads, ϵ is in the range of 0.01 to 0.1. This range of values of ϵ is chosen to ensure that hydrophobic interactions between alkyl tails are close to thermal energy.¹⁶ The well-depth of the 9-3 potential for interaction between polar head groups and surface is chosen to be $\epsilon = 5$. This ϵ_s is chosen to match the strong affinity of polar head group with the metal surface to the values obtained from previous density functional theory (DFT) calculations.¹⁷ The number of beads in an inhibitor molecule is kept at 20 beads (1 polar head bead and 19 hydrophobic beads). All simulations are performed using the Large-scale Atomic/Molecular Massively Parallel Simulator (LAMMPS) MD simulations package.¹⁸ For each data point, the simulations are performed in parallel on eight processors or on a Graphic Processing Unit (GPU). Equilibrium is obtained after 3×10^9 to 4×10^9 MD time-steps.

RESULTS

Importance of Hydrophobic Interactions between Alkyl Tails in Facilitating Adsorption

It is often assumed that the driving force of adsorption of inhibitor molecules is mainly the strong polar-metal surface affinity, and the role of alkyl tails is only to repel water and ionic species from reaching the metal surface. To ascertain the validity of this assumption, we performed a series of simulations wherein the hydrophobic interactions between the alkyl tails of inhibitor molecules were systematically varied by changing the well-depth of LJ interaction, ϵ , while the interaction between the polar head group and metal surface was kept the same ($\epsilon_s = 5$). A small value of ϵ corresponds to weak affinity between the tails of corrosion inhibitor molecules, while a large value corresponds to strong affinity.

Figure 1 shows the total number of adsorbed corrosion inhibitor molecules, N , on the metal surface as a function of ϵ . Interestingly, it is observed that when the hydrophobic interactions between tails (ϵ) are small, only weak, random adsorption occurs. As the hydrophobic interactions are increased (Figure 1(a)), a significant increase in the adsorption amount is seen. At the point of highest adsorption formation of a self-assembled monolayer (SAM) is observed. At even larger values of ϵ , the molecules start aggregating in the bulk, and the adsorbed amount decreases. (Figure 1 (b) and (c)). These results indicate that the hydrophobic interactions between inhibitor tails play an important role in the adsorption of inhibitor molecules at the metal-water interface, contrary to the traditional point-of-view.

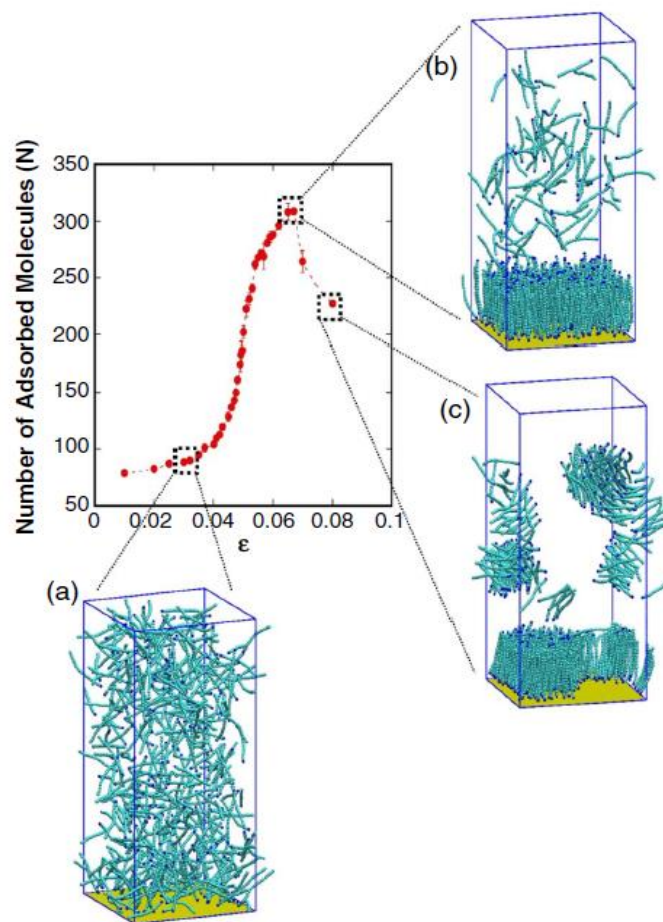


Figure 1: The number of adsorbed molecules in equilibrium, N , as a function of the strength of hydrophobic interactions between inhibitor tails, ϵ . Snapshots of the simulation system at different ϵ values are also shown: (a) $\epsilon = 0.03$: low, random adsorption; (b) $\epsilon = 0.065$: adsorbed SAM; and (c) $\epsilon = 0.08$: aggregated states in the bulk and the adsorbed phases.

Aggregated and Adsorbed Morphologies of Corrosion Inhibitor Molecules

To study the effect of molecular geometry on the adsorption behavior, corrosion inhibitor molecules with a larger polar head were studied. The size of the polar group bead was changed to $\sigma_p = 2\sigma$. Figure 2(a) and (b) shows the aggregation observed of corrosion inhibitor molecules in the bulk state, that is, in the absence of a surface. Figure 2(c) and (d) shows aggregation of molecules on the surface. From the figures, it is found that depending on their shape, inhibitor molecules aggregate in both bulk and adsorbed states as micelles of different geometries. When the size of the polar bead is same as that of the alkyl bead (σ), a planar micelle is observed both in the bulk and the adsorbed states. So, a self-assembled monolayer is observed when these molecules adsorb on the surface. For a larger head group ($\sigma_p = 2\sigma$), the inhibitor molecules form micelles of cylindrical shape.¹² These results indicate that molecular geometry plays an important role in deciding the morphologies of the adsorbed corrosion inhibitor films and a bulk polar head group may not be as effective in forming a SAM.

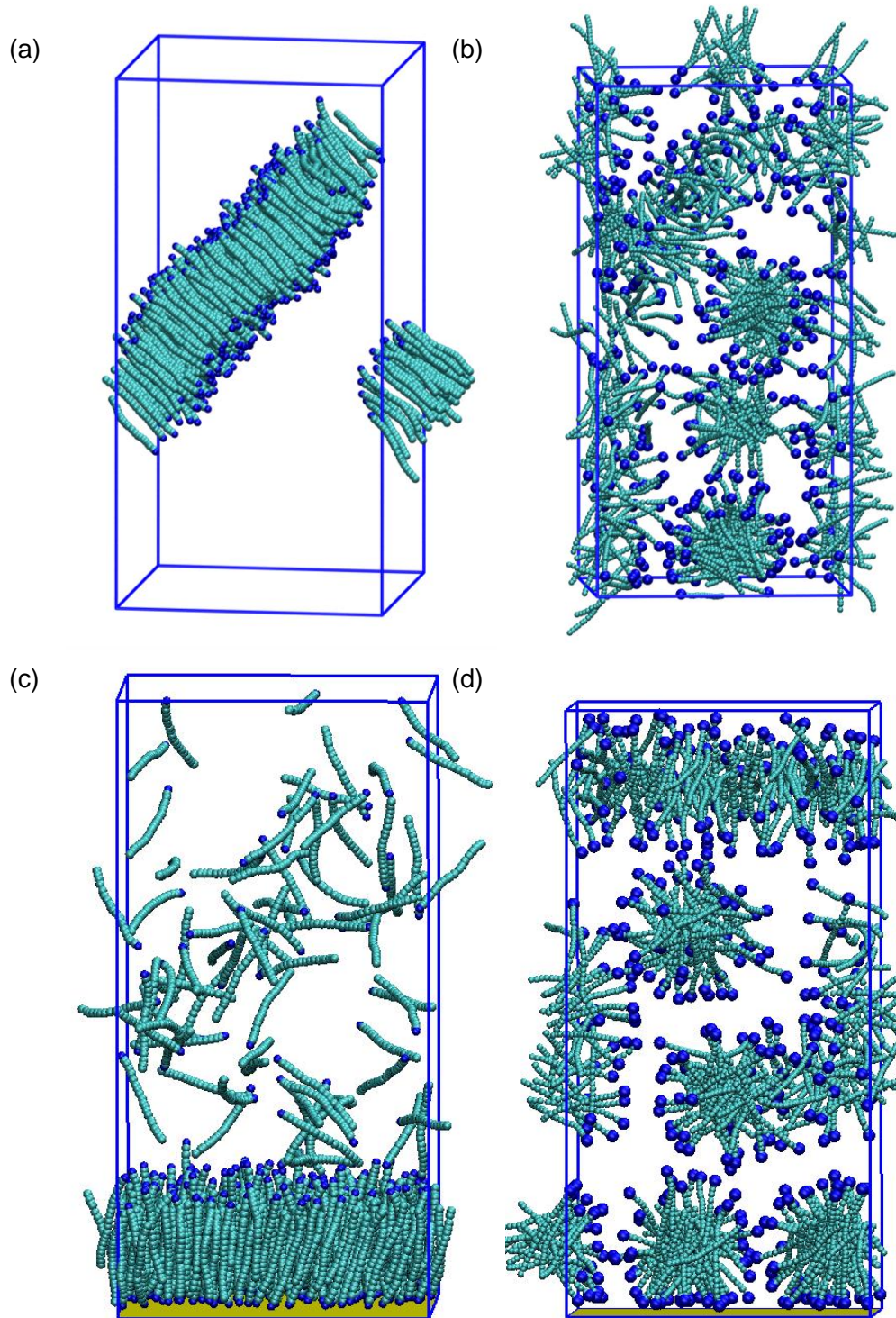


Figure 2: Aggregation of corrosion inhibitor molecules in the bulk (a) as a planar micelle for $\sigma_p = \sigma$, and (b) as a cylindrical micelle for $\sigma_p = 2\sigma$. Adsorption of corrosion inhibitor molecules (c) as a SAM for $\sigma_p = \sigma$, and (d) as cylindrical micelles for $\sigma_p = 2\sigma$.

Affinity between Polar Head Group and Surface changes Nature of the Adsorbed Inhibitor Film

We find that in our system, the adsorption of corrosion inhibitor molecules occurs in three stages (Figure 3).¹⁴ In the first stage, most inhibitor molecules quickly adsorb onto the surface with their polar group towards surface. This is due to the strong interaction between surface and polar head group. In the second stage, the rate of adsorption is slower, and some molecules adsorb with their polar group pointing away from the surface. In the last stage, no further increase in the molecules adsorbed with their polar group towards surface is observed and molecules only adsorb with their polar head group pointing away from surface. In the last stage, adsorption is driven by lateral hydrophobic interactions between the tails.

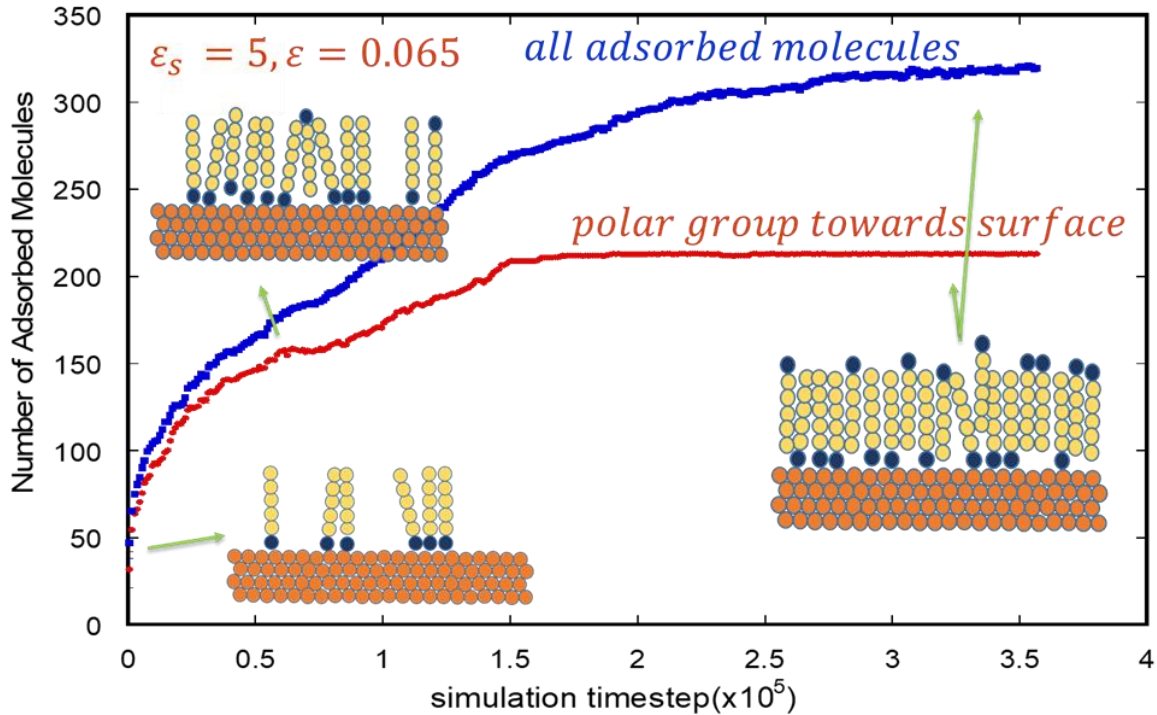


Figure 3: Kinetics of adsorption of corrosion inhibitor molecules. The red curve shows adsorption of molecules with their polar group towards the surface. The blue curve shows total number of adsorbed molecules. Adapted with permission from Sharma et al.¹⁴

In all the results discussed above, the affinity between the surface and the polar head group is $\epsilon_s=5$, which represents strong affinity between inhibitor and metal surface. To study how this affinity affects adsorption, we have varied the strength of ϵ_s in the simulations. The interaction between the hydrophobic tails is kept at $\epsilon=0.065$. Figure 4 shows kinetics of adsorption with different values of ϵ_s . From figure 4, it is observed that upon reducing the strength of ϵ_s , the rate of adsorption is reduced for both the first and the second stages. However, we find that the overall equilibrium adsorption amount does not vary significantly, indicating that a SAM of similar packing density is formed. This is because the adsorption is dictated by lateral hydrophobic interactions between alkyl tails and not by the affinity of the polar group with the surface.

Figure 5 shows the number of molecules adsorbed with their polar group towards the surface as a function of time for the same simulation trajectories as in Figure 4. Here, it is found that the equilibrium adsorption amount is different for different values of ϵ_s . This indicates that the affinity between the polar head group and surface changes the fraction of molecules adsorbed with polar group toward surface, and thus changes the nature of the adsorbed corrosion inhibitor film. A weaker affinity will result in less molecules adsorbed with their polar group towards surface, and thus a less hydrophobic film.

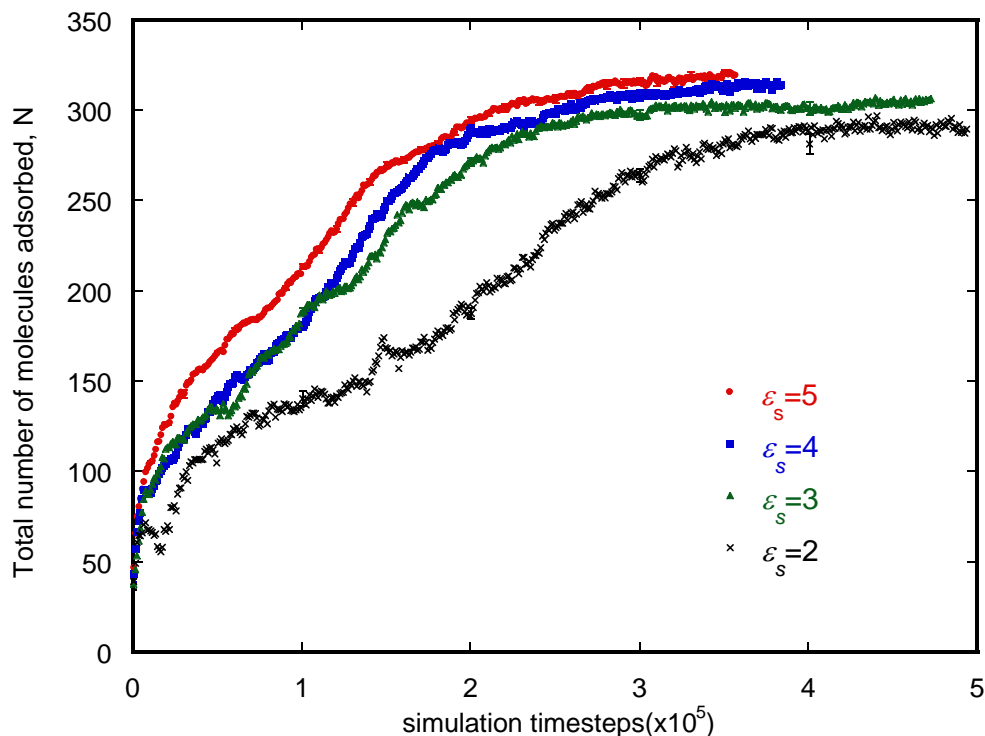


Figure 4: Total number of molecules adsorbed as a function of simulation time for different values of the affinity between polar head group and metal surface, ϵ_s .

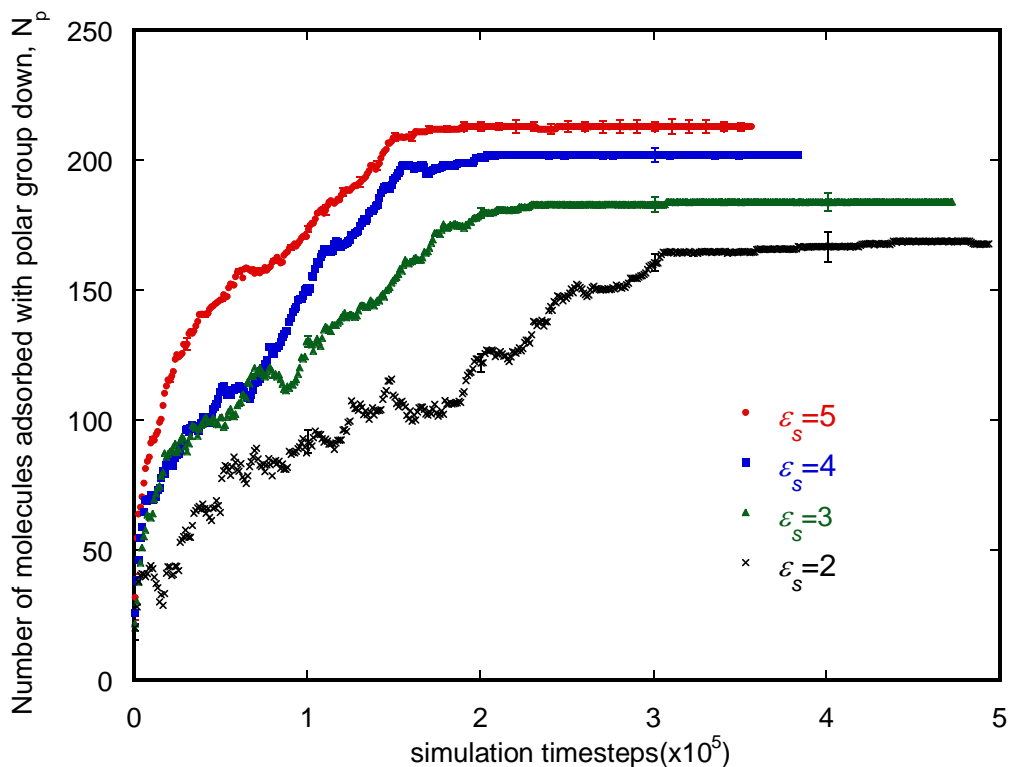


Figure 5: Number of molecules adsorbed with their polar group towards the surface as a function of simulation time for different values of affinity between the polar head group and metal surface, ϵ_s .

Entrainment of Oil in Adsorbed Corrosion Inhibitor films

Previous research work has revealed that presence of an oil phase or oil wetting of the surface improves corrosion inhibition efficiency of inhibitor molecules.¹¹ While researchers have speculated this improved performance to co-adsorption of inhibitor and oil molecules at the metal-water interface, there is no molecular-level interpretation of this result.

In this section, we have studied how the presence of linear oil molecules affect the adsorption behavior of corrosion inhibitor molecules. For simplicity, we have only focused on oil molecules which are as long as the alkyl tail of the corrosion inhibitor molecules. That is, they comprise of 19 hydrophobic beads. While we acknowledge that the results will be a function of the nature of oil, such an extensive study will be part of future work. Now, our simulation system comprises of equal molar amounts of corrosion inhibitor molecules and oil molecules. Figure 6 shows the total number of molecules adsorbed in equilibrium. We have studied two different corrosion inhibitor molecules, $\sigma_p = \sigma$ and $\sigma_p = 2\sigma$. For both cases, we find that oil molecules are entrained in the adsorbed inhibitor film. This entrainment is due to the lateral hydrophobic interaction between the tails of inhibitor molecules and oil molecules. An interesting and non-intuitive result is that a significant increase in the number of adsorbed molecules is seen in the case of $\sigma_p = 2\sigma$ in the presence of oil. We find that due to the presence of oil, the cylindrical morphology of the adsorbed molecules in the case of $\sigma_p = 2\sigma$ is altered. The entrained oil molecules change the adsorbed morphology and a SAM is formed. This dramatic change in the adsorbed morphology results in significant increase in the adsorbed amount. Thus, this result shows that the presence of oil molecules can help in improving the adsorption characteristics of inhibitor molecules.

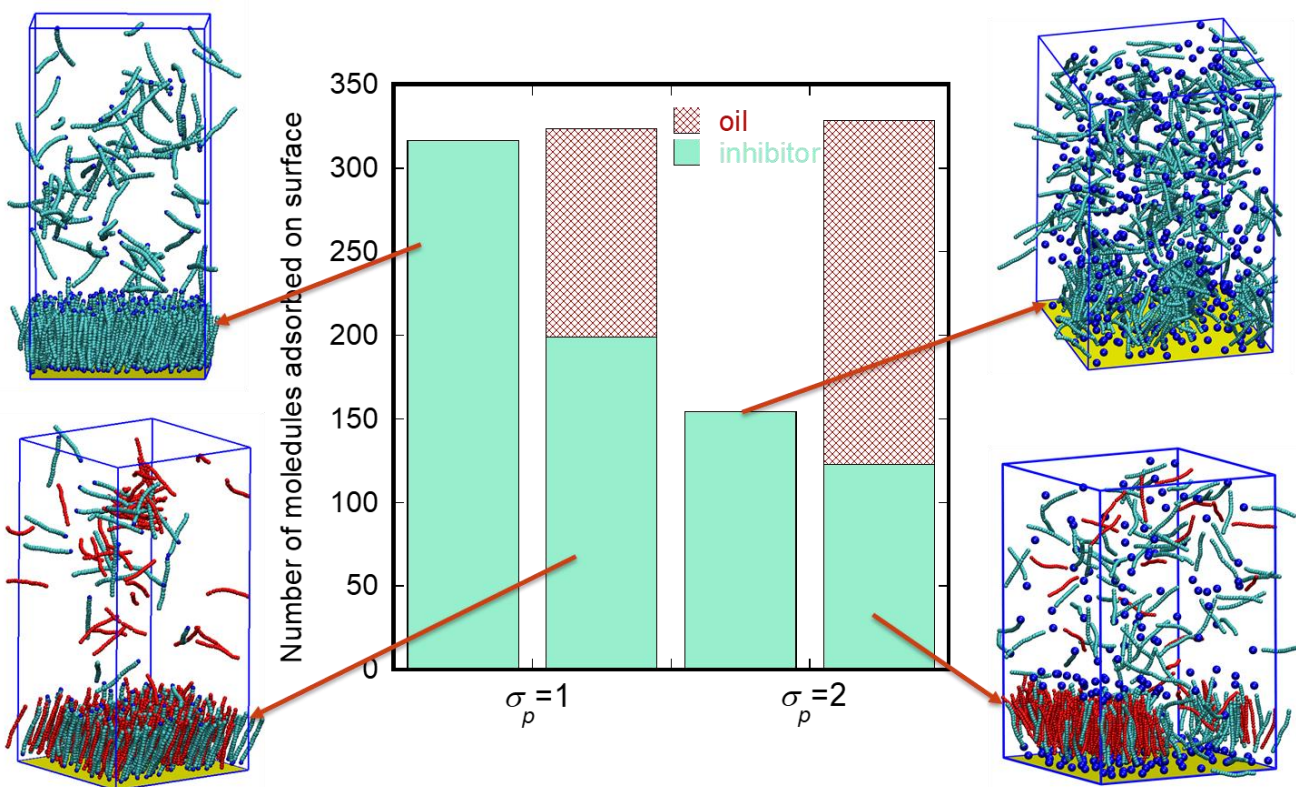


Figure 6: The number of adsorbed molecules in equilibrium for $\sigma_p = \sigma$ and $\sigma_p = 2\sigma$ and snapshots of respective system.

CONCLUSIONS

In this project, we have employed classical molecular simulations to study adsorption and self-assembly of corrosion inhibitor molecules on surfaces. We report that (a) in addition to forming a hydrophobic layer and repel water; alkyl tails of inhibitor molecules play an important role in the adsorption and self-assembly process. (b) The geometry of inhibitor molecules dictates adsorbed morphologies of inhibitor films. (c) metal-polar head group interactions change the nature of adsorbed corrosion inhibitor films. Total number of molecules absorbed into a SAM does not change with affinity of metal surfaces and polar head group, but the overall hydrophobic character of the film decreases with decrease in the metal-polar head interaction strength. We also report that even though oil molecules do not have any affinity for the metal surface, they get entrained in the adsorbed layer through lateral hydrophobic interactions between oil molecules and alkyl tails of inhibitor molecules. Entrainment of oil molecules in adsorbed corrosion inhibitor films may result in a dramatic change in the morphology of the films, wherein cylindrical micelles formed by pure inhibitor molecules are transformed into a planar SAM on the surface.

ACKNOWLEDGEMENTS

This research was supported by the NSF CBET grant 1705817. The authors thank researchers at the Institute for Corrosion and Multiphase Technology (ICMT) for useful discussions. XK thanks the support of Ohio University Graduate College Fellowship for the year 2018-2019. Computational resources for this work were provided by the Ohio Supercomputer Center. Additional computational resources from National Science Foundation XSEDE grant number DMR190005.

REFERENCES

1. M.B. Kermani, A. Morshed, *Corrosion* 59, 8 (2003): p. 659-683.
2. A.J. McMahon, *Colloid Surface* 59, (1991): p. 187-208.
3. M. Finšgar, J. Jackson, *Corros. Sci.* 86, (2014): p. 17-41.
4. M. Shalaby, M. Osman, *Anti-Corrosion Methods and Materials* 48, 5 (2001): p. 309-318.
5. J.A. Martin, F.W. Valone, *Corrosion* 41, 5 (1985): p. 281-287.
6. Y. Duda, R. Govea-Rueda, M. Galicia, H.I. Beltran, L.S. Zamudio-Rivera, *J. Phys. Chem. B* 109, 47 (2005): p. 22674-22684.
7. A. Edwards, C. Osborne, S. Webster, D. Klenerman, M. Joseph, P. Ostovar, M. Doyle, *Corros. Sci.* 36, 2 (1994): p. 315-325.
8. X. Liu, S. Chen, F. Tian, H. Ma, L. Shen, H. Zhai, *Surf. Interface Anal.* 39, 4 (2007): p. 317-323.
9. Y.-J. Tan, S. Bailey, B. Kinsella, *Corros. Sci.* 38, 9 (1996): p. 1545-1561.
10. A. Edwards, C. Osborne, S. Webster, D. Klenerman, M. Joseph, P. Ostovar, M. Doyle, *Corros. Sci.* 36, 2 (1994): p. 315-325.
11. Y. Xiong, B. Brown, B. Kinsella, S. Nešić, A. Pailleret, *Corrosion* 70, 3 (2013): p. 247-260.
12. X.Y. Ko, S. Sharma, *J Phys Chem B* 121, 45 (2017): p. 10364-10370.
13. J.D. Weeks, D. Chandler, H.C. Andersen, *The Journal of chemical physics* 54, 12 (1971): p. 5237-5247.
14. S. Sharma, X.Y. Ko, Y. Kurapati, H. Singh, S. Nestic, *Corrosion* 75, 1 (2019): p. 90-105.
15. M.P. Allen, D.J. Tildesley, *Computer Simulation of Liquids*, Oxford university press, 1989).
16. N. Choudhury, B.M. Pettitt, *J. Am. Chem. Soc.* 127, 10 (2005): p. 3556-3567.
17. N. Kovacevic, I. Milosev, A. Kokalj, *Corros. Sci.* 124, (2017): p. 25-34.
18. S. Plimpton, *J Comput Phys* 117, 1 (1995): p. 1-19.